

The National Ignition Facility: Ushering in a new age for high energy density science

E. I. Moses, R. N. Boyd, B. A. Remington, C. J. Keane, and R. Al-Ayat

Citation: *Physics of Plasmas* **16**, 041006 (2009); doi: 10.1063/1.3116505

View online: <https://doi.org/10.1063/1.3116505>

View Table of Contents: <http://aip.scitation.org/toc/php/16/4>

Published by the [American Institute of Physics](#)

Articles you may be interested in

[The physics basis for ignition using indirect-drive targets on the National Ignition Facility](#)

Physics of Plasmas **11**, 339 (2004); 10.1063/1.1578638

[Development of the indirect-drive approach to inertial confinement fusion and the target physics basis for ignition and gain](#)

Physics of Plasmas **2**, 3933 (1995); 10.1063/1.871025

[Point design targets, specifications, and requirements for the 2010 ignition campaign on the National Ignition Facility](#)

Physics of Plasmas **18**, 051001 (2011); 10.1063/1.3592169

[Direct-drive inertial confinement fusion: A review](#)

Physics of Plasmas **22**, 110501 (2015); 10.1063/1.4934714

[Review of the National Ignition Campaign 2009-2012](#)

Physics of Plasmas **21**, 020501 (2014); 10.1063/1.4865400

[Three-dimensional HYDRA simulations of National Ignition Facility targets](#)

Physics of Plasmas **8**, 2275 (2001); 10.1063/1.1356740



ADVANCES IN PRECISION
MOTION CONTROL

READ NOW

Piezo Flexure Mechanisms
and Air Bearings

PRESENTED BY

PI

The National Ignition Facility: Ushering in a new age for high energy density science

E. I. Moses, R. N. Boyd, B. A. Remington, C. J. Keane, and R. Al-Ayat

Lawrence Livermore National Laboratory, Livermore, California 94550, USA

(Received 2 September 2008; accepted 29 December 2008; published online 22 April 2009)

The National Ignition Facility (NIF) [E. I. Moses, *J. Phys.: Conf. Ser.* **112**, 012003 (2008); <https://lasers.llnl.gov/>], completed in March 2009, is the highest energy laser ever constructed. The high temperatures and densities achievable at NIF will enable a number of experiments in inertial confinement fusion and stockpile stewardship, as well as access to new regimes in a variety of experiments relevant to x-ray astronomy, laser-plasma interactions, hydrodynamic instabilities, nuclear astrophysics, and planetary science. The experiments will impact research on black holes and other accreting objects, the understanding of stellar evolution and explosions, nuclear reactions in dense plasmas relevant to stellar nucleosynthesis, properties of warm dense matter in planetary interiors, molecular cloud dynamics and star formation, and fusion energy generation. © 2009 American Institute of Physics. [DOI: [10.1063/1.3116505](https://doi.org/10.1063/1.3116505)]

I. INTRODUCTION

The National Ignition Facility (NIF)^{1–3} located at Lawrence Livermore National Laboratory (LLNL) is the largest laser ever built. NIF is expected to produce ignition in laser driven inertial confinement fusion (ICF) by delivering sufficient laser energy to compress and heat a millimeter (radius) sized pellet of ²H and ³H (D and T) sufficiently that the two nuclei will fuse to produce ⁴He, a neutron, and 17.6 MeV of energy per reaction.^{4,5} Construction of NIF was completed in March 2009. A National Ignition Campaign (NIC), a series of experiments to optimize the parameters associated with producing ignition, is poised to start.⁶ Other participants in the NIC are Los Alamos and Sandia National Laboratories, the University of Rochester Laboratory for Laser Energetics (LLE), General Atomics, Inc., and the Naval Research Laboratory. Although NIF is a research facility, a successful ignition demonstration may well have implications for the design of future energy sources.

Besides the goal of achieving ignition, NIF will support programs associated with stockpile stewardship.⁷ The conditions that NIF can produce will simulate those inside stars and planets sufficiently closely to also provide compelling motivation for experiments in basic high-energy-density (HED) science, especially in astrophysics and planetary physics.

NIF joins a number of other facilities that are currently performing experiments in HED Science. These include, for example, the OMEGA (Ref. 8) and OMEGA EP (Ref. 9) facilities at the LLE, the Jupiter Laser Facility¹⁰ at LLNL, the ZR Magnetic Pinch Facility at Sandia National Laboratory,¹¹ and the Trident Laser Facility¹² at Los Alamos National Laboratory. New facilities in various stages of construction or design are the Laser MegaJoule¹³ (LMJ) in France, the HiPER,¹⁴ or High Power Laser Energy Research, Facility in the United Kingdom, FIREX-I,¹⁵ or Fast Ignition Realization Experiment, at the Institute for Laser Energetics (ILE) in Japan, and the Shenguang laser¹⁶ in China.

II. DESCRIPTION OF THE NATIONAL IGNITION FACILITY

A. Basic description of NIF operation

The beams from NIF begin with nanojoule sized pulses from a solid state laser. Its pulses are divided into 48 beams and passed through preamplifiers.³ Those beams are subsequently divided further into a total of 192 beams, each about 40 cm square in profile, that pass six times through Nd glass amplifiers, ultimately achieving a total of 4 MJ of 1051 nm laser light. These 192 beams are transported in sets of four (“quads”) to a target chamber, at which potassium dihydrogen phosphate (KDP) crystal sheets convert the 1051 nm (1ω) light first to 526 nm (2ω) light, then in a second KDP crystal to 1.8 MJ of 351 nm (3ω) light. This ultraviolet light then enters a 10 m diameter target chamber, where the beams are focused onto the inside walls of a *Hohlraum*, a centimeter sized cylinder made of gold and uranium that houses the DT spherical pellet, and is located at the center of the target chamber. The laser light produces x rays inside the *Hohlraum* that ablate the shell of the pellet, which then heats and compresses the DT fuel to a temperature and density of several $\times 10^8$ K and several hundred g cm⁻³, which should produce ignition. Under these conditions, the DT in the pellet should fuse to produce more than 10 MJ of energy and 10¹⁹ neutrons over 10–100 ps.^{5,6} A sketch of the NIF is given in Fig. 1. Its current status is described at the NIF website.⁷

B. Technological advances at NIF

A number of technological advances have gone into making NIF an operating facility. As noted above, the laser beams pass through the main amplifiers and the power amplifiers a total of six times before entering the target chamber. A key advance was the optical switch, called the “plasma electrode pockels cells (PEPCs),” large planar electrodes that can have their polarization transmission direction switched by changing the voltage across them.¹⁷ Electrical connections to the surfaces are achieved with a plasma on either

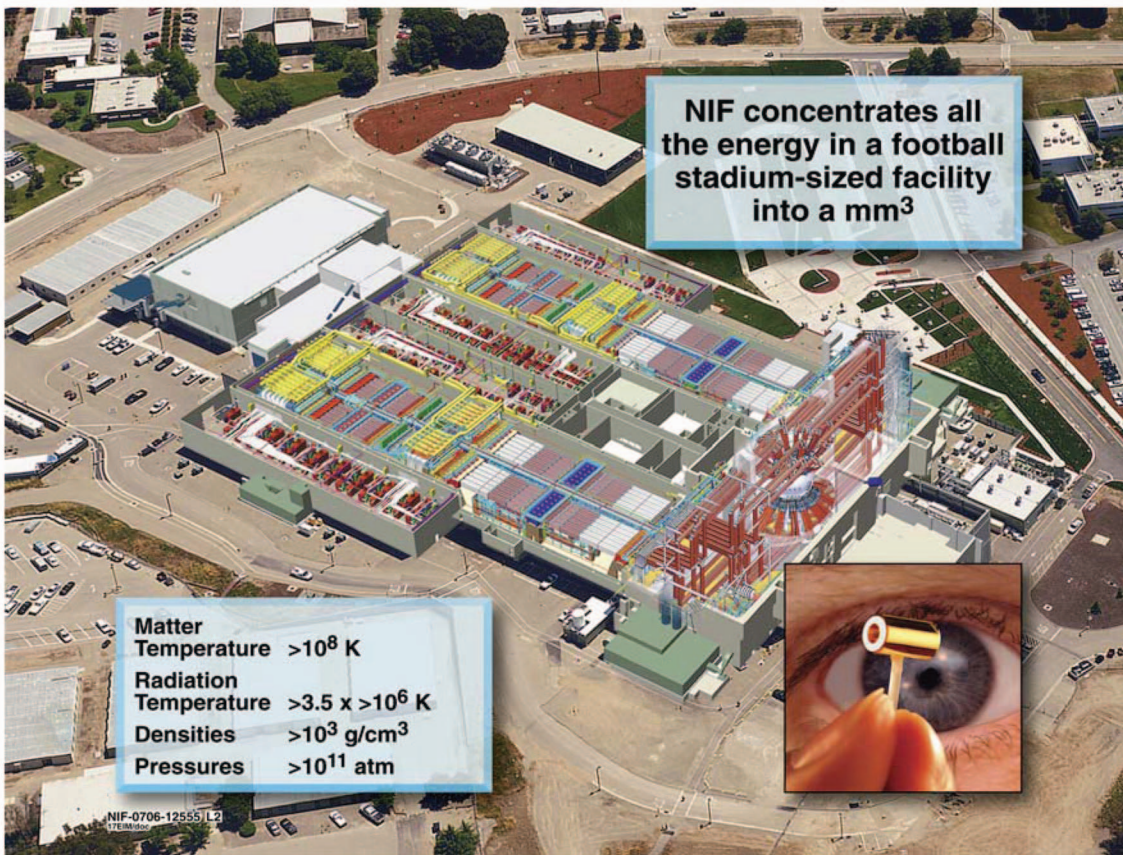


FIG. 1. (Color) Schematic view of the National Ignition Facility. The main amplifiers occupy about half the building at the upper left, whereas the target chamber is at the lower right (Refs. 3 and 6).

side of each cell. Since the laser beams are polarized, the PEPCs are set so their initial polarization direction allows transmission. When they are switched to the other direction, following four passes through the main amplifiers, the beams are directed to the target chamber. The multiple passes through the main amplifiers allow NIF to be considerably smaller than a single pass facility would have been.

Major effort has gone into minimizing damage to the laser components from the intense beams passing through them. It was found that a huge reduction in damage could be achieved by making the glass surfaces as impurity-free as possible. In-house annealing of damaged spots can in most cases be achieved and the damaged component put quickly back into service. In addition, creating precision “microshadows” located over incipient damage spots allows the laser to continue to be operated at high fluences while minimizing the growth of existing damage spots.³

The targets also represent a major advance in technology. A cutaway sketch of a target is shown in Fig. 2. Targets are fabricated with a beryllium or plastic outer shell (ablator) and a cocktail of elements in shells interior to that. The DT is put into the hollow spheres as a gas, then frozen out in a layer that adheres to the inside of the innermost shell (which requires a cryogenic system that is inserted into the NIF target chamber). This necessitates a thin, 10 μm diameter, fill tube. It has been found that the frozen shells can be made very smooth, at least for a few hours, a result of the heating

by the decays of the radioactive tritium. Every step of target fabrication has to produce extremely smooth, precisely characterized surfaces to preserve the spherical geometry to as large an extent as possible.

All the components of NIF must work in concert to make a successful ignition shot. Extensive computer simulations of every phase of the NIF shot sequence have been run to select the optimal laser pulse shape (see Fig. 3), pointing, *Hohlräum* design, optimum mixture of elements in the shell of the target, and a number of other variables.¹⁸ Many more simulations have been run to determine such parameters as the required alignment accuracy of the target (10 μm) and the maximum allowed deviations from sphericity of the implosion.

C. NIF diagnostics

In addition to achieving ignition, NIF is designed to understand the ignition process in detail.^{4,5} To this end a number of diagnostics (detector systems) have been developed to produce the information necessary to achieve this understanding. While these will not be described in detail (much more detail is given on the NIF website⁷), some general features are as follows. Because beam and target alignment are so critical to optimal ignition, several devices to monitor these aspects of NIF are in place. Both soft and hard x-ray detectors will characterize the conditions inside the *Hohlräum*.

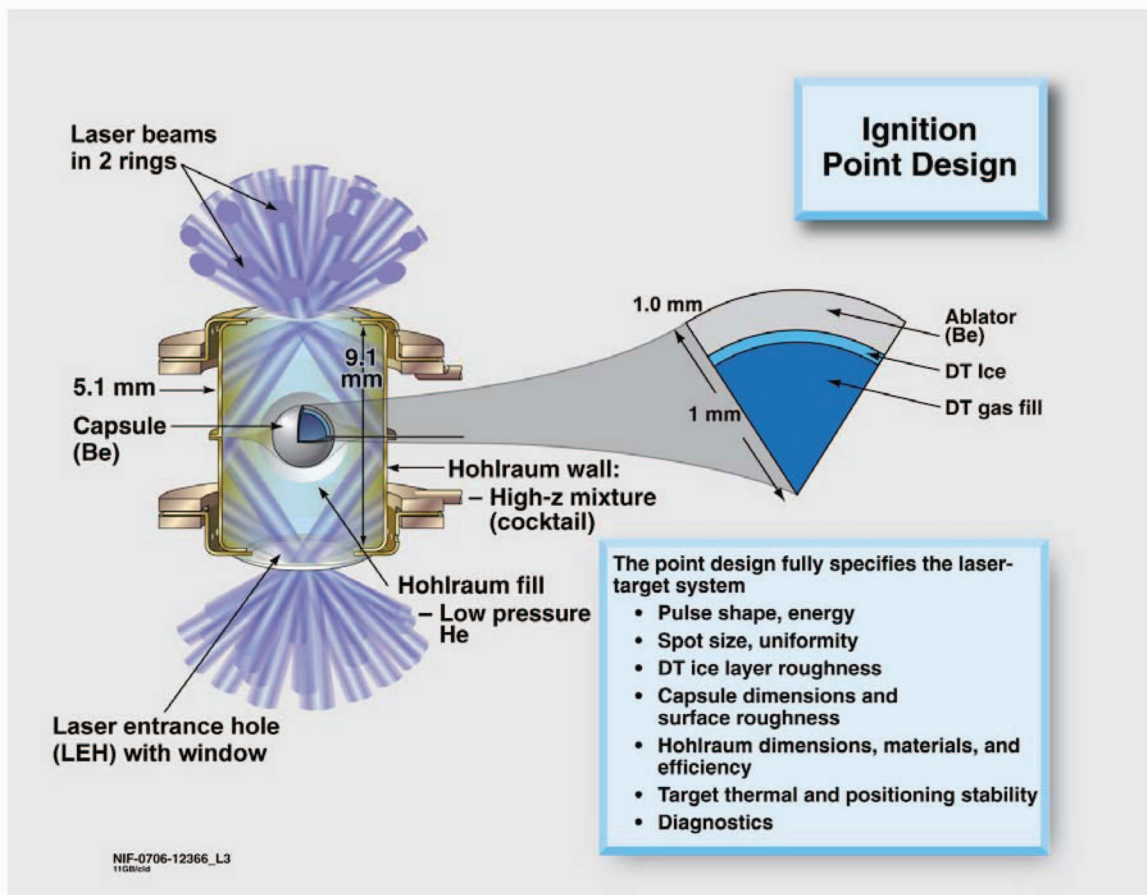


FIG. 2. (Color) Cutaway view of a NIF target, showing the various layers of ablator, the frozen DT shell, and the gaseous DT interior.

raum necessary to produce the target implosion. Another diagnostic samples the 1051 nm light that emerges from the NIF amplifiers to measure its energy, timing, and pulse shape. Several types of neutron detectors are being designed to monitor the output from ignition shots. A radiochemical analysis system is being designed to analyze the products of the ignition, or the yields from nonignition, shots.

Another diagnostic designed to observe the compressed DT fuel directly is called the advanced radiographic capability (ARC).¹⁹ The ARC diagnostic system typically refers to a “backlighter” plate or wire onto which the ARC petawatt beams can be directed to produce high energy x rays for radiographically imaging the target. This diagnostic will be used in ignition experiments and for many of the basic science experiments to be described below.

Many of these diagnostic devices are designed to be inserted in the NIF target chamber via diagnostic insertion modules (DIMs), which are large vacuum interlocks into which the diagnostic devices can be inserted, pumped out, and opened to the target chamber. These devices are described in greater detail on the NIF website.⁷

D. Other aspects of ICF

The mode in which NIF will first attempt to achieve ignition is indirect drive, in which the laser beams are used to heat the inside of a *Hohlraum*, which then generates the x rays that heat the pellet and cause the implosion. There are other possible modes by which the laser energy could be coupled to the target. Direct drive, in which the laser beams impinge directly onto the pellet, is being developed by LLE, NRL, and ILE to try to achieve ICF. Direct drive has the advantage of coupling a greater fraction of the laser energy to the pellet, but is sensitive to beam spot nonuniformities

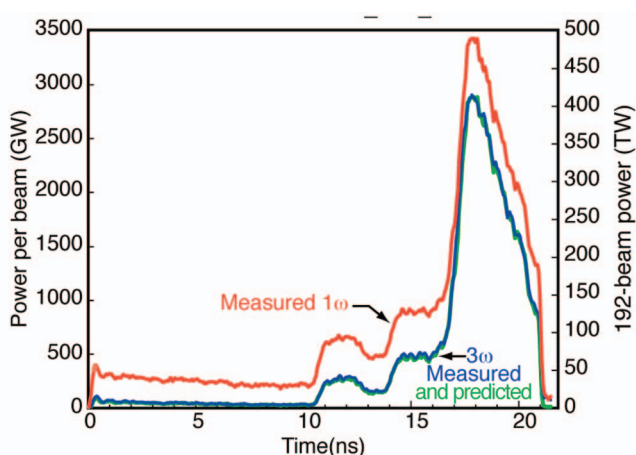


FIG. 3. (Color) The NIF laser pulse, chosen to optimize the many parameters that can affect successful ignition, that will be delivered to the target. As can be seen, the measured and predicted pulses are essentially in perfect agreement.

(“imprinting”). Research at LLE emphasizes sophisticated beam smoothing techniques to create a direct drive option.²⁰

Another mode of coupling laser energy to the DT pellet is fast ignition.^{21,22} Here the long pulse drive laser is used to compress the fuel. When the fuel reaches maximum compression, a short intense laser pulse is directed at the center of the pellet, generating a hot electron “spark.” This mode of ICF was first proposed by Tabak *et al.*²¹ and is now the topic of a major international effort. This approach is the central focus of the Japanese group that is now building FIREX I and also constitutes the assumed ICF mode in HiPER, being built in the United Kingdom. A major component of OMEGA EP will also focus on fast ignition. Fast ignition is thought to provide a way of achieving ICF with a considerably smaller primary laser than NIF. There are still many questions associated with fast ignition, however, so attempts to achieve ICF in that way are several years farther into the future than the hot spot ignition approach that will constitute the first efforts at NIF. It should be noted that the ARC setup described above will be able to provide the short pulse capability for NIF also to attempt fast ignition experiments.

III. SCIENCE USES OF NIF

During ignition the environment inside a NIF ignition capsule is expected to reach temperatures in excess of 10^8 K, densities approaching 1000 g cm^{-3} , pressures in excess of 10^{11} atm , and neutron densities in excess of $10^{26} \text{ neutrons cm}^{-3}$, albeit for very short times (as short as 20 ps). These extraordinary temperatures and densities are seven times the values at the core of the Sun. Indeed, conditions such as these define the emerging field of HED science. The goals for this field have been stated in a series of high level reports: The Science and Applications of Ultrafast, Ultra-intense Lasers;²³ Frontiers in High Energy Density Science, The X-Games of Contemporary Science;²⁴ Connecting Quarks with the Cosmos;²⁵ and Report of the Interagency Task Force on High Energy Density Physics.²⁶

These studies will ultimately be used to establish the priorities for basic research experiments to be run on NIF. Since the focus of this article is primarily laboratory astrophysics, it is also worth noting that several review articles have been written over the past two decades addressing this subject area as it can be pursued using high-power lasers and Z-pinches.^{27–31} In the sections below we review and update several of these areas, specifically in the context of NIF.

A. Burning plasmas

NIF will enable studies of nuclear reactions in conditions relevant to nucleosynthesis in stars and supernovas, as well as the physics of hot, ultradense plasmas. This will create research opportunities that cannot be duplicated in accelerator experiments or in any other laboratory setting. Ignition experiments should provide conditions relevant to reactions in stellar interiors and supernova explosions, thereby enabling investigations of the effects of ultrahigh density hot plasmas on nuclear reaction rates. Generating and characterizing such extreme plasma conditions, and developing the required diagnostics to study the science of burning plasmas,

however, present daunting challenges. Progress in this area will require diagnostic techniques capable of characterizing the rapidly evolving plasma conditions in the harsh environment of a burning plasma. Promising avenues include ultrafast x-ray spectroscopy, imaging, and burn time evolution measurements.³²

Because of the extremely high densities, $\rho_{\text{fuel}} > 100 \text{ g/cm}^3$, and electron temperatures, $T_e > 20 \text{ keV}$, in igniting capsules, a unique set of conditions exists in calculating the x-ray emission of ignited capsules. The enormous densities will produce Stark broadened lines even for very tightly bound heavy ions, which can in principle be used to measure electron densities in the target. Accurate calculations of the plasmas conditions will be made using relativistic non-LTE atomic physics codes such as CRETIN.³³

Once ignition is achieved, the intense burst of DT neutrons, generating a flux of $10^{32}–10^{33} \text{ neutrons}/(\text{cm}^2 \text{ s})$, may allow excited state nuclear reactions to occur, which are relevant to the nucleosynthesis of the heavy elements, i.e., those nuclei more massive than Fe.³⁴ It may also be possible to study thermonuclear reactions in highly screened, dense plasmas, relevant to reactions in dwarf stars. Finally, if high gain ($G > 100$) implosions can be produced,³⁵ it may be possible to examine some of the physics issues surrounding the proposed deflagration-to-detonation transition, and the role of hydrodynamic mixing, relevant to type Ia supernovas.³⁶

B. Instabilities and hydrodynamics

NIF appears to be ideally suited to study turbulent hydrodynamic instabilities. As noted above, these have been studied in the context of ICF for several decades.^{37–41} They have many similarities to the instabilities that can occur in stars, especially in supernovas.⁴² For example, a recent paper⁴³ reports on studies of several types of instabilities that can occur in type Ia supernovas, and another⁴⁴ on instabilities in core collapse (type II) supernovas. These should both be quite amenable to study in scaled experiments on NIF. Typical parameters that will be achieved at NIF include flow Reynolds numbers $> 10^6$, Peclet numbers $> 10^3$, and shock Mach numbers > 10 .

The topic of properly scaled experiments is particularly important. Ryutov *et al.*⁴⁵ worked out the scaling for several different regimes, the simplest being “Euler scaling,” for which we give an example. In the simplest case the Reynolds number and Peclet number are large and both radiation and magnetic fields are negligible. In comparing the dynamics in the exploding star and the laboratory setting, assume that spatial scale, density, and pressure differ by factors of a , b , and c . Then if the time scales are adjusted to differ by a factor of $\sim a(b/c)^{1/2}$, the two systems will evolve identically up to the point at which the underlying assumptions break down. These types of scaling criteria allow a wide variety of dynamic phenomena in astrophysics to be studied in HED laboratory experiments.

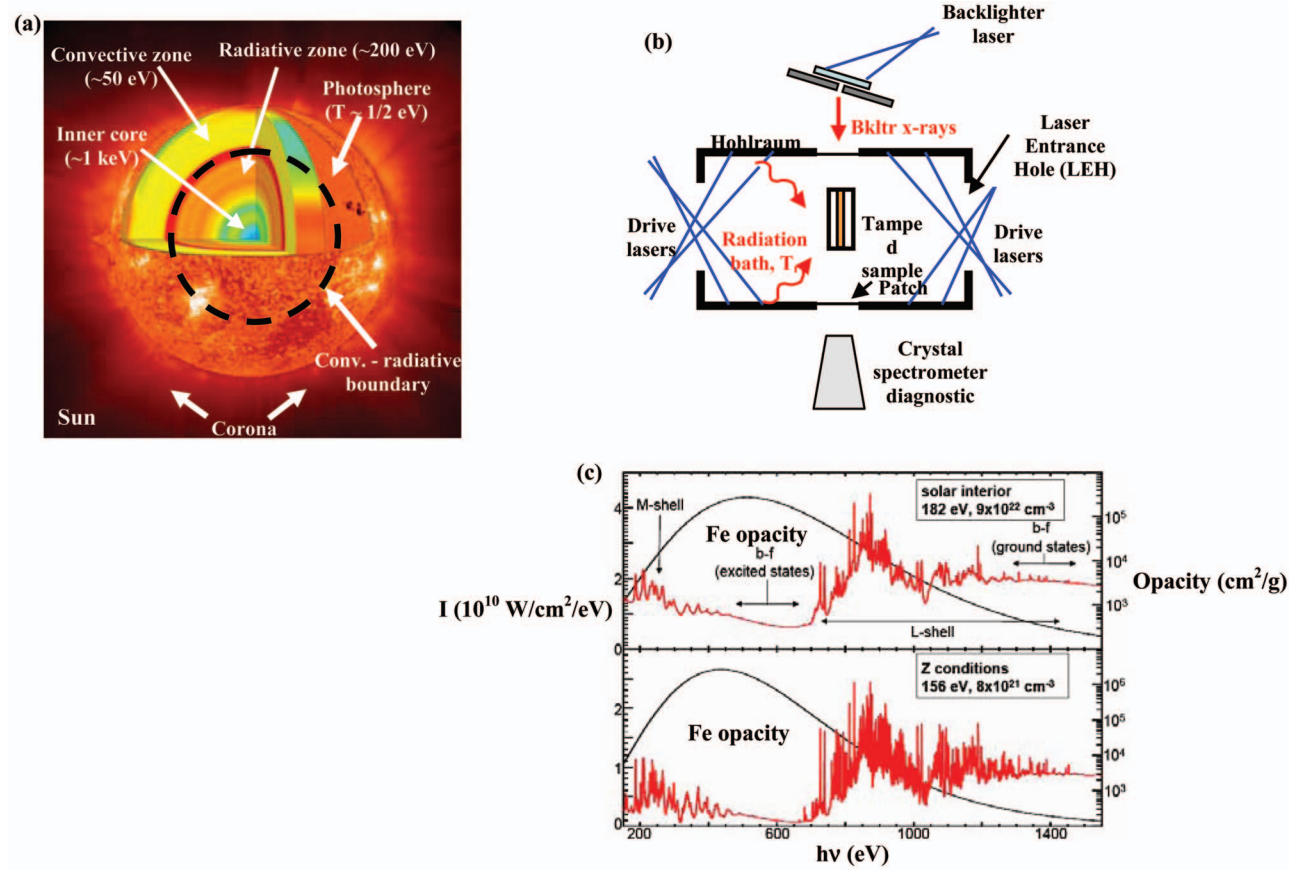


FIG. 4. (Color) (a) Schematic of the solar interior (from <http://www.solarviews.com/eng/sun.htm>). (b) Schematic showing a laser driven, radiatively heated, opacity experiment. (c) Calculated Fe opacities for the solar interior in the radiative zone (top) and for the conditions of an opacity experiment on the Z magnetic pinch facility (bottom) (Ref. 58).

C. Opacities

Understanding the stars, how they are born, live, die, and are reborn, has historically been and remains an overarching goal of astrophysics and astronomy. Sophisticated models⁴⁶ and simulations^{47,48} of stellar evolution exist, fully three-dimensional in some cases,^{49–51} yet discrepancies remain with observations, even with our closest star, the sun. For example, predictions of the location of the boundary separating the radiative and convective zones in the solar interior differ with the observational result deduced from high precision helioseismology.^{52–54} One question is whether the opacities used in these stellar models are accurate.

The conditions that prevail in the solar interior are indicated schematically in Fig. 4(a). At the core of the sun, where the nuclear burning is most intense, the densities are $\sim 100 \text{ g/cm}^3$, and temperatures exceed $T_e \sim 1 \text{ keV}$. At the surface (photosphere), the temperatures are much lower, $T_e \sim 1/2 \text{ eV}$. A key region in the solar interior is the boundary between the radiative zone in the deep interior and the convective zone in the outer regions of the sun. Interior to this boundary, heat is transport outward from the core by radiative transport (as opposed to hydrodynamic flow or convection). Near this boundary, the conditions of temperature and electron density are thought to be $T_e \sim 180\text{--}200 \text{ eV}$ and $n_e \sim 10^{23} \text{ cm}^{-3}$. Models of the sun and stars require complex opacities, such as the opacity of Fe, under the conditions

ranging from $T_e \sim 100\text{--}1000 \text{ eV}$, and densities ranging from $n_e \sim 10^{23}\text{--}10^{26} \text{ cm}^{-3}$, spanning solar interior conditions from the convective zone down to the core.

A schematic for a generic opacity experiment is shown in Fig. 4.^{55–57} Here, lasers are used to heat the *Hohlraum*, generating a quasiblackbody radiation cavity. The sample to be measured is tamped between layers of CH to maintain a uniform density. This sample is heated in the radiation bath, which causes it to expand (decompress). At the appropriate time, a continuum source of backlighter x rays is passed through the sample. The backlighter x rays that pass through the sample are spectrally dispersed in a crystal spectrometer and recorded. From this transmission spectrum, the opacity as a function of photon energy can be inferred. High quality opacity measurements can also be made on a pulsed power, magnetic pinch facility such as Z. The basics of what is described above still hold.

Figure 4(c) shows calculations of the opacities of Fe at the radiative-convective boundary of the sun, namely, $T_e = 182 \text{ eV}$ and $n_e = 9 \times 10^{22} \text{ cm}^{-3}$. The predicted spectrum for Fe at $T_e = 156 \text{ eV}$ and $n_e = 8 \times 10^{21} \text{ cm}^{-3}$, is also shown, which corresponds to the conditions of recent opacity measurements on Fe made at Z.⁵⁸ The enormous complexity and detail in the bound-bound transition lines in the open L-shell of Fe at these conditions is immediately apparent. Accurate models of stellar interiors require accurate opacity simula-

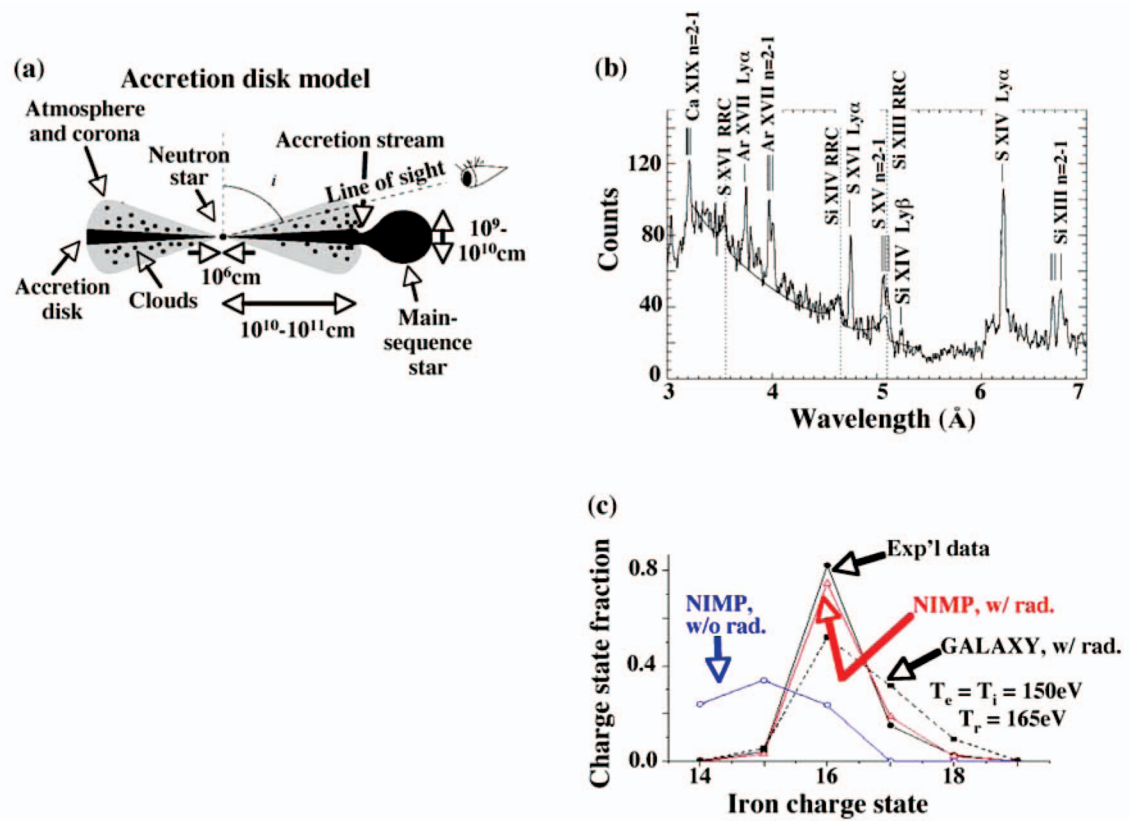


FIG. 5. (Color) (a) Schematic showing the assumed configuration of a low-mass x-ray binary, corresponding to a neutron star accreting matter from an accretion disk “fed” from a companion main-sequence star (Ref. 62). (b) Chandra x-ray spectrum from Cygnus X-3 x-ray binary (Ref. 63). (c) Calculations and experimental data of a photoionized plasma experiment done on the Z magnetic pinch facility (Ref. 65).

tions of Fe and the other stellar constituents, in all this complexity, and this will require experiments at relevant conditions against which to compare. The measurements of Fe made at Z have already shown that the opacity models used in the standard solar model are not able to reproduce the experimental measurements done on the Z facility sufficiently well.⁵⁸ These experiments marked a major step forward, but were made under conditions that still were not at sufficiently high density and temperature to reproduce conditions in the radiative zone of the sun. Reaching conditions relevant to the radiative zone, $T_e > \sim 200$ eV and $n_e > \sim 10^{23}$ cm⁻³, will require the NIF laser. It is anticipated that such high density, high temperature opacity measurements will be one of the focus areas for experiments on NIF in the future.⁵⁹

D. Photoionized plasmas

One of the most intriguing objects in the universe is an accreting compact object, such as a neutron star or black hole. At the extreme is an accretion disk around a massive black hole (10^8 – $10^9 M_{\odot}$) at the center of a galaxy such as the active galactic nucleus (AGN) object NGC 4261.⁶⁰ Another much closer example is Cyg X-3, an accreting x-ray binary system.⁶¹ A sketch of an accreting neutron star compact object in a binary system with a main-sequence star is shown in Fig. 5(a).⁶² An example spectrum from the accreting binary x-ray source Cyg X-3 is shown in Fig. 5(b).⁶³

These spectra result from the photoionized plasma created by the enormous continuum x-ray flux that results as the matter from the accretion disk falls inward onto the compact object. In this case, radiative excitation, absorption, and emission processes dominate, and collisional processes are negligible. The emission-line spectrum of the x-ray binary Cygnus X-3 is consistent with recombination-dominated line formation. From this it is inferred that the source of energy “pumping” the lines is the hard x-ray continuum. The simplest interpretation of Cyg X-3 assumes that the x-ray emission is from plasma in photoionization equilibrium.

To check or calibrate the models used to interpret these spectra, experimental data of photoionized plasmas in relevant regimes are required. It was recognized recently that similar conditions of photoionized plasmas could be created in the laboratory using the intense burst of x rays coming from the z-pinch at the SNLA Z-facility.⁵⁹ An experiment was developed to measure the photoionized plasma x-ray spectra under nearly scaled conditions. The radiation from the pinch created an 8 ns FWHM, 120 TW, $T_r = 165$ eV near-blackbody radiation source.⁶⁴ A number of photoionized plasma models have now been compared with the results of this laboratory experiment. Experimental and observed ionization distributions for an iron plasma are shown in Fig. 5(c).⁶⁵ A radiation temperature of $T_r = 165$ eV, electron temperature of $T_e = 150$ eV, and electron number density of $n_e = 2 \times 10^{19}$ cm⁻³ were assumed for the calculations with the

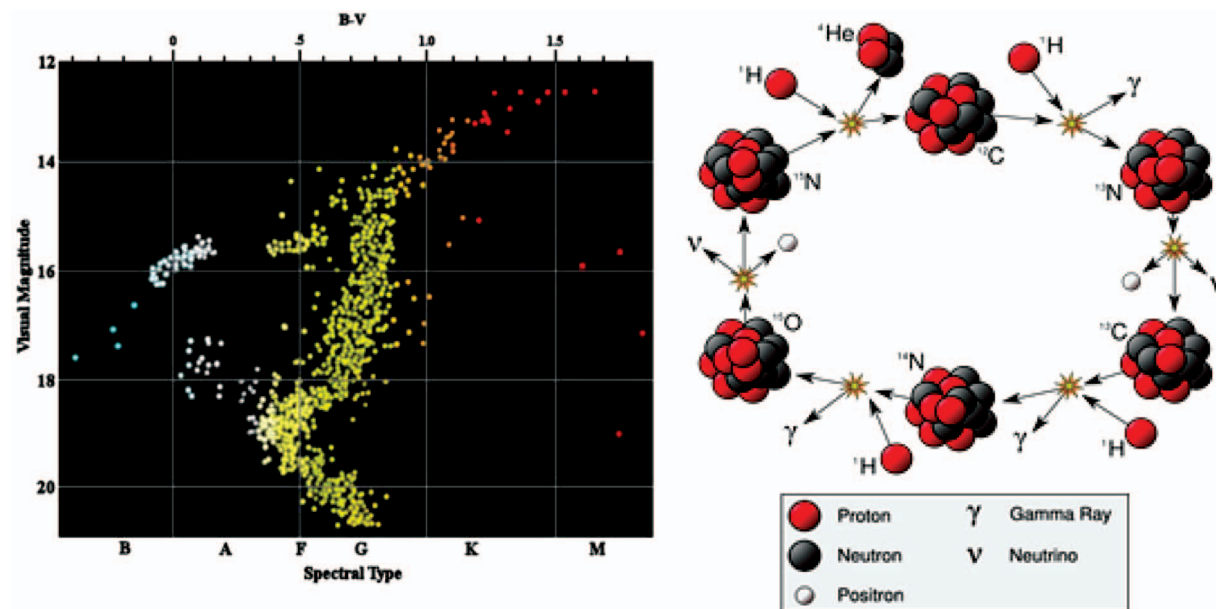


FIG. 6. (Color) Several aspects of the $^{14}\text{N}(p, \gamma)^{15}\text{O}$ reaction, including the reactions of the primary cycle of CNO burning reactions on the right, and the H-R diagram for globular cluster M3 on the left. From Ref. 67.

average-atom model NIMP. The observed ionization state would be underpredicted by calculations without the inclusion of the radiation field, which is a central feature of astrophysical photoionized plasmas. Also included in the comparison are predictions from the more detailed model GALAXY presented for the same conditions. Good agreement with experiment is found only for the calculations that include the radiation field, but collisional effects are not completely negligible. The average-atom model is observed to be quite effective at calculating these photoionized plasma x-ray spectra, which is an important conclusion because of its wide use in modeling laboratory plasmas.

To study scaled systems relevant to compact object (neutron stars, black holes) accretion disks requires a low density, radiation dominated, photoionized plasma. An exceedingly high flux of thermal x rays is needed so that, in the surrounding plasma, atomic excitations, ionization, and recombination processes are dominated by the radiation field, with the effects from electron-ion collisions being negligible. On NIF, creating these intense x-ray luminosities should be possible, allowing models of photoionized plasmas, relevant to accreting black holes, to be checked and calibrated, in a properly scaled experimental testbed.

E. Nuclear astrophysics

The temperature and density that will be achieved in the NIF pellet are sufficiently similar to those in stars that NIF should have applications in nuclear astrophysics, i.e., in measuring some of the nuclear reactions that occur in stars, but that have been difficult to measure, or for which discrepancies exist in data sets. Simulations suggest that the yields achievable at NIF will permit measurement at the temperatures that are relevant to stars, and that the similarity of the conditions of the NIF target to those in stars will greatly

simplify the corrections that need to be made to accommodate the electron screening at the low energies at which these measurements are made.

Although a number of nuclear reactions have been discussed as possibilities for study at NIF, two deserve particular attention. The first, $^{14}\text{N}(p, \gamma)^{15}\text{O}$, associated with hydrogen burning in stars,⁶⁶ is of special interest to cosmology. The second is actually a general class of reactions that involve nuclear reactions in high temperature environments; the case discussed here is relevant to the astrophysical s-process.

1. The $^{14}\text{N}(p, \gamma)^{15}\text{O}$ reaction

The $^{14}\text{N}(p, \gamma)^{15}\text{O}$ reaction is the slowest reaction in the main hydrogen burning cycle that occurs in massive stars. Therefore, it is the reaction that determines how long such stars burn hydrogen in their cores. This has interesting implications to the globular clusters, clusters of millions of stars that all appear to have been created at the same time early in the history of our galaxy. When the luminosities of these stars are plotted against their surface temperature (their Hertzsprung–Russell diagram; see Fig. 6), there is a sharp kink in that plot at magnitude ~ 19 .⁶⁷ This kink identifies the most massive stars that have consumed their core hydrogen, so have completed that phase of their evolution. Use of a stellar evolution code then can determine the ages of those stars, and hence provide a lower limit on the age of the universe.⁶⁸ The $^{14}\text{N}(p, \gamma)^{15}\text{O}$ reaction is crucial to that determination.

A recent measurement of this reaction⁶⁹ found that its rate was only 60% of the rate that had been accepted for many years. However, there are some difficult corrections that need to be made to obtain the reaction rate that goes into the stellar evolution codes from the measured data. Because

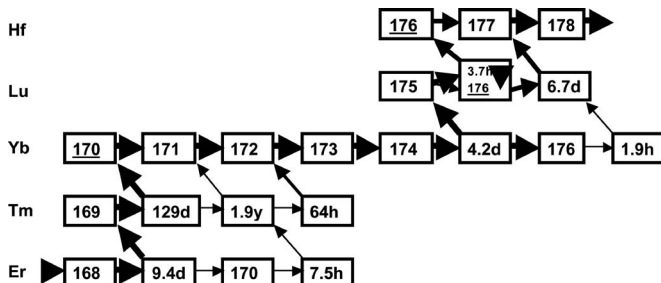


FIG. 7. s-process pathway from ^{168}Er to ^{178}Hf . Alternate pathways, that is, branch points, exist for both the Tm and Lu nuclei, among others. The widths of the arrows indicate the strength of that flow. At ^{175}Lu , neutron capture goes primarily to the ^{176}Lu isomeric state, which populates the ground state, which then undergoes a subsequent neutron capture to ^{177}Lu .

of the importance of this rate to both cosmology and our understanding of stellar evolution, it is important that a re-measurement of this rate be made by an independent technique. NIF will provide a unique opportunity in this regard. The NIF target for this experiment could be ammonia: NH_3 .

2. Measuring (n, γ) cross sections in a high temperature environment

The slow neutron capture or s-process of nucleosynthesis synthesizes half the nuclei heavier than iron.^{66,70} Its main component (which makes $A > 100$ nuclei) acts in the helium burning shells of asymptotic giant branch (AGB) stars, which, because of the different hydrodynamic processes and nuclei involved, stabilize at two temperatures $k_B T = 8$ and 30 keV, thus creating two essentially discrete temperatures for the s-process. The s-process proceeds via a series of (n, γ) neutron capture reactions and β -decays until an unstable isotope is synthesized that has a long enough lifetime (typically > 1 year) that the (n, γ) rate competes with β -decay rate. This produces a “branch point,” as illustrated in Fig. 7; these nuclei provide information about the stellar temperature and density during the s-process.

Low-lying excited states of the branch point nuclei can be excited in the hot s-process plasma; this can produce a much different *effective* β -decay lifetime than would exist for the ground state nuclei.⁷¹ However, there may also be a significant effect on the (n, γ) reaction rate resulting from the population of low-lying excited states; excited states can have very different (n, γ) reaction rates compared to ground state nuclei. This can cause significant changes in the *effective* (n, γ) reaction rates. Although extensive measurements of (n, γ) cross sections for stable nuclei along the s-process pathway⁷² exist, few cross sections on branch point nuclei, and especially on excited state nuclei, have been measured.⁷³ In the cases in which cross sections on excited (isomeric) state nuclei have been measured or estimated, the resulting cross sections were generally much different from those on the ground states. This leads to large differences in the thermally averaged cross sections, and large effects on the s-process abundances over those that include just the ground state nuclei.⁷⁴

The conditions in an imploded NIF target ($k_B T \approx 2\text{--}12$ keV and \approx several hundred g/cm³) are very similar to those found in an AGB stellar interior. The low-energy

($E_n < 1$ MeV) neutron fluence in these non-DT targets, of order of 10^{17} neutrons/cm², is approximately 10^{10} times higher than that found in the stellar interior, thereby subjecting a tracer nucleus to an equivalent neutron exposure of $\sim 300+$ years duration in an AGB stellar interior. Thus an (n, γ) cross section measurement relevant to the s-process could be performed by adding branch point nuclei to a NIF target. These, together with their (n, γ) reaction product nuclei, could be collected, following the NIF shot, and their ratio used to determine the cross section.

As seen in Fig. 7, the thulium isotopic chain produces two s-process branch points ($^{169,171}\text{Tm}$), both of which are radioactive and which lead to radioactive reaction products ($^{170,172}\text{Tm}$ respectively). Furthermore, ^{171}Tm has a first excited state at 5.025 keV that would certainly be significantly populated in an AGB stellar interior. Thus this would be an excellent, and important, case for study.

F. Planetary interiors

The ability of NIF to produce extraordinarily high pressures at relatively low temperatures (warm dense matter) creates the potential for condensed matter scientists and planetary scientists to study states of matter that have never been accessed before. Specifically, the conditions that exist within the interiors of massive planets such as Jupiter and Saturn become accessible for study, as do phase changes that can occur in solids at pressures never before achievable in the laboratory.

Measurements on the planets Jupiter and Saturn have made it possible to test our understanding of the formation and structure of giant planets, at least within the context of the things we know about matter at extremely high pressure. The planets are thought to be formed at relatively high temperature, then to cool with time, as can be seen on the left hand side of Fig. 8. This figure also shows the calculated temperatures for Jupiter and Saturn assuming a “homogeneous evolution model.”⁷⁵ It is seen to give an excellent description of Jupiter’s surface temperature, but fails badly for Saturn, which in this model is predicted to cool much too rapidly. Indeed, it appears from this model that Saturn is only half the known age of the solar system of 4.5 GYr.

However, calculations in which a new evolutionary model is assumed for Saturn that permits phase separation between hydrogen and helium to form helium droplets that will settle to the core of the planet (see right hand side of Fig. 8) produced the two additional curves on the left hand side of Fig. 8; that of Fortney and Hubbard⁷⁶ appears to produce the correct result for the temperature of Saturn. This would be consistent with the observation that helium appears to be depleted in the surface of Saturn.⁷⁷

Models of planetary interiors are very sensitive to the fundamental properties, such as equation of state (EOS) and conductivity, of their constituent elements, such as hydrogen and helium for the gas giant planets,⁷⁸ water and methane for the ice giants, and iron for the terrestrial planets. Experiments to measure these fundamental properties of matter in regimes relevant to planetary interiors have been under development for over a decade. Recent results from experi-

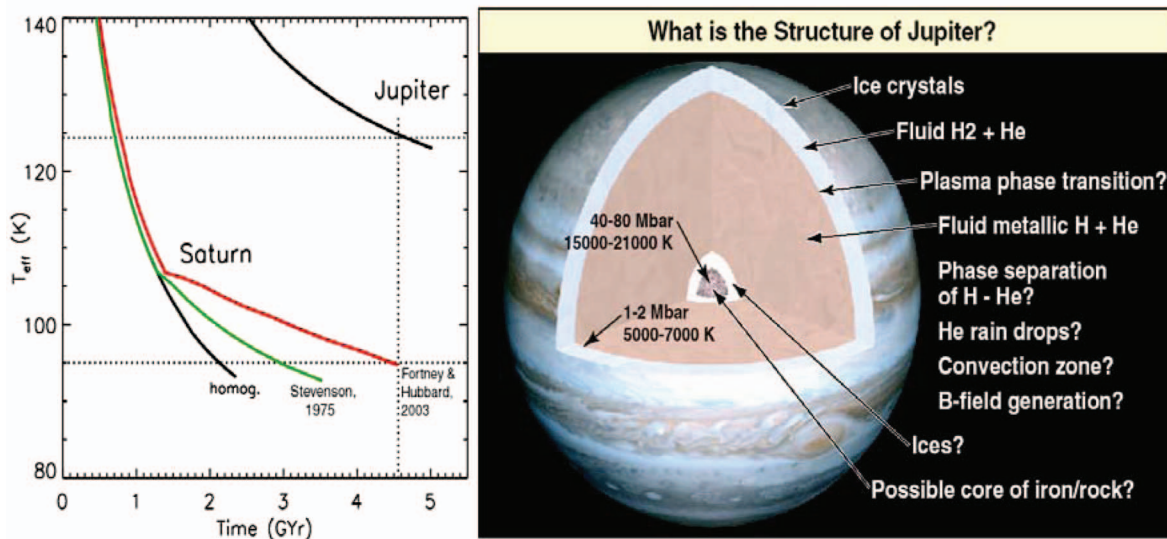


FIG. 8. (Color) Cooling curves, on the left, for Jupiter and Saturn in the homogeneous evolution model (Ref. 76) along with modifications, for Saturn, from a model in which helium is assumed to rain out of the mixed hydrogen-helium phase (seen for Jupiter on the right). The helium apparently forms rain drops that settle to the center of the planet at high pressure. Left hand figure courtesy of J. Fortney.

ments conducted on the Omega laser have measured Hugo-niot data for high pressure, dense helium,⁷⁹ the shock induced transformation of liquid hydrogen into a metallic fluid,⁸⁰ and electronic conduction in shock-compressed water.⁸¹ Additionally, high pressure, shock compressed iron has been measured on the LULI and Vulcan lasers,⁸² and the shock compressed EOS of liquid hydrogen has been measured on the Z magnetic pinch facility.⁸³

With NIF, experiments could be done, for the first time, to measure the EOS of planetary constituents at pressures approaching those at the centers of the giant planets. This would allow models of planetary interiors to be tested throughout the full range of relevant conditions, from surface to core.

G. Condensed matter physics

With the advent of HED experimental facilities, new regimes of high pressure materials science have become accessible. Macroscopically, ultrahigh compression can change a material's mechanical properties such as the yield strength, tensile strength, ductility, and toughness. Microscopically, ultrahigh compression changes the atomic lattice arrangement of a material. Under compressions of $V/V_0 < 0.5$, where V_0 is the sample ambient volume, all elements and alloys are likely to undergo structural phase transitions.⁸⁴⁻⁸⁶ At high compressions the valence electron orbitals become distorted and start to interact (become "hybridized") with the inner orbitals. Sophisticated theoretical approaches now exist to predict the phases of matter under these conditions, yet the predictions differ by factors of several, from theory to theory. Crystal structure data at pressures over a few Mbars are essentially absent; this field of experimental science remains largely untouched. To achieve ultrahigh compression in the solid state, a near-isentropic ramp-loading technique has been developed that maintains the sample material well below the melting point, as shown schematically in Fig. 9(a).⁸⁷

An example of ramp wave loading profiles up to a maximum pressure, $P_{\max} \sim 2$ Mbars, developed on OMEGA is shown in Fig. 9(b).⁸⁸ It is possible on the OMEGA laser, using this drive, for example, to compress solid-state samples by up to a factor of 2, i.e., $V/V_0 \sim 0.5$ or $\rho/\rho_0 \sim 2$. With ramp wave drives to be developed on NIF, peak pressures of over 20 Mbars, and compressions of $V/V_0 \sim 0.2-0.3$ or $\rho/\rho_0 \sim 3.5$ in the solid state should become possible.⁸⁹

Once ultrahigh pressures in the solid state are accessed, dynamic diffraction becomes a diagnostic technique that allows a time-dependent probe of the lattice structure to be recorded as the material is being compressed. This technique has been developed to date on crystal samples that have been shocked compressed, as opposed to ramp wave compressed. This technique is illustrated schematically in Fig. 9(c). Shock compressed results for single crystal Fe are shown in Fig. 9(d) for a $P_{\text{shk}} \sim 200$ kbars shock along the (002) crystal lattice direction.^{90,91} In this case, one clearly sees the Bragg diffraction arcs from the uncompressed (002) lattice planes in the bcc phase (bcc_0), the elastically compressed (002) lattice planes in the bcc phase (bcc_1), and the hcp (2110) lattice planes after the α - ϵ phase transition (hcp). Of particular note is that the time resolution of this technique is determined by the duration of the pulsed backlighter x rays, which can be very short, < 1 ns, and possibly as short as ~ 1 ps, as set by the x-ray burst duration driven by the short pulse laser.⁹²⁻⁹⁵ A second lattice diagnostic, dynamic extended x-ray absorption fine structure (EXAFS), has also been developed.⁹⁶ This EXAFS technique probes the lattice short range order, works with polycrystalline or single crystal samples, and offers the potential to infer phase, compression, and temperature of the compressed sample, with subnanosecond time resolution. Based on spectroscopy of the transmitted x rays from a continuum backlighter source, just above an absorption K -edge in the sample of interest, this K -shell dynamic EXAFS technique has been developed on the Omega laser. Figure

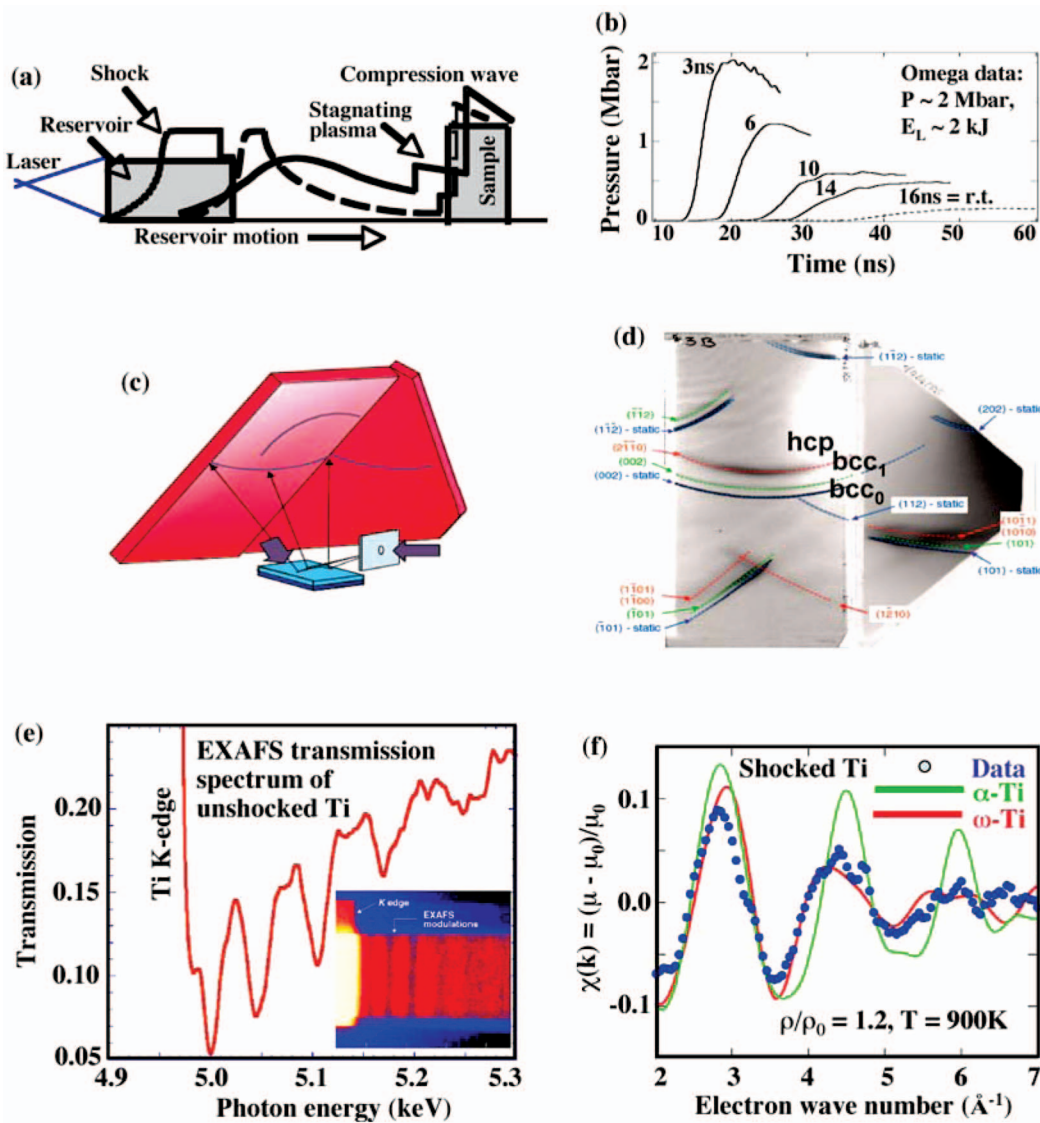


FIG. 9. (Color) (a) Sketch showing the configuration for a ramp wave, applied pressure vs time (“drive”) (Ref. 87). (b) Results from measurements of this ramp wave drive, showing pressure vs time for five different experiments done on the OMEGA laser facility (Ref. 88). (c) Sketch showing the configuration for a laser driven, dynamic diffraction experiment (Ref. 90). (d) Results from a dynamic diffraction experiment on shocked Fe done on the Omega laser facility (Refs. 90 and 91). (e) EXAFS transmission spectrum from unshocked, room-temperature Ti. The inset shows the raw image (Ref. 96). (f) Shocked EXAFS spectrum (plotting symbols), overlaid with two FEFF8 theoretical curves, corresponding to 20% compression with no phase transition, and 20% compression with the $\alpha \rightarrow \omega$ phase transition (red curve). (Reproduced, with modifications, from Ref. 97.)

Figure 9(e) shows the “raw” transmission spectrum for unshocked titanium. The fine structure above the absorption K -edge at 4.75 keV can be modeled with theory to infer compression, temperature, and phase. Figure 9(f) shows the analyzed EXAFS result for shocked Ti.⁹⁷ The best fit theoretical curve clearly indicates that at shock pressures $>\sim 120$ kbars, the Ti has undergone the α -to- ω phase transition, over time scales <1 ns. Shocked iron has also been studied with dynamic EXAFS, and also shows the α - ϵ phase transition at shock strengths $P_{\text{shk}} > 130$ kbars.⁹⁸ Finally, dynamic EXAFS has been demonstrated in a ramped compression wave, such as shown in Figs. 9(a) and 9(b).⁹⁹ These two techniques, dynamic diffraction and EXAFS, allow the lattice to be probed in detail, even at extreme conditions of pressure and compression. Future work will develop these lattice diagnos-

tic techniques to work at very high (ramped) pressures, so that new phases of matter at ultrahigh pressures, $P_{\text{max}} \gg 1$ Mbar, can be investigated.^{89,100}

IV. CONCLUSIONS

The National Ignition Facility laser, which has just been completed, will provide over a megajoule of energy in a cubic millimeter of volume on nanosecond time scales. Although the best ideas for frontier science on NIF are likely yet to emerge, we have described in this brief report a few areas that seem fertile for additional consideration.

Stars are born out of molecular clouds or “stellar nurseries,” often incubated by the intense radiation from nearby young stars. The dynamics of the radiation-driven evolution

of these molecular clouds, such as the Eagle Nebula, are rich with possibilities for scaled experiments on NIF. Once formed, stars are heated by nuclear fusion in the interior and cooled by radiative emissions at the surface. Opacities control the rate at which heat moves from the core to the surface to be radiated away. Opacity measurements at the relevant conditions of density and temperature possible on NIF are very important to understanding stellar evolution. Supernova explosions mark the deaths of massive stars by mechanisms still not fully understood. Scaled experiments on shock-driven explosion dynamics that simulate some of the processes that occur in supernovae will be possible on NIF. Stars are also the thermonuclear furnaces for building the Periodic Table of elements. The reactions occur under highly screened conditions in the dense plasmas of the stellar interior. During a supernova explosion, the enormous flux of particles and radiation can lead to a rapid succession of nuclear reactions occurring potentially from both ground states and excited states of the nucleus. Both regimes of nucleosynthesis can potentially be accessed on NIF. Thermonuclear reactions in highly screened plasma at relevant temperatures can be achieved using nonignition capsules, and experiments using the ignition flux of neutrons and radiation may be able to study successive reactions on very short time scales on NIF.

Accreting black holes are among the most exotic and interesting objects in the universe. Understanding the dynamics of matter near a black hole as it spirals inwards toward the hole is an enormous scientific challenge. It is possible to recreate the conditions of radiation dominated photoionized plasmas to test the relevant models on NIF, thereby firming up our interpretations of the astronomical x-ray data being returned to earth by the space-borne observatories such as Chandra and XMM.

In one of the major developments in astronomy this decade, nearly 300 exoplanets, that is, planets outside of our solar system, have been discovered. Hence there is intense interest in understanding how planets are formed and understanding properties, such as their interior structures. NIF will allow experiments that test key aspects of the very high-pressure physics that determines the interior structures of the planets down to their cores, both in our solar system and outside it.

NIF can also be used to quasi-isentropically place matter in states of extremely high pressure but low enough temperature that it stays solid. Under such extreme pressures the basic phases, structures, and properties of solid-state matter are very uncertain due to the lack of experimental data. There are a wide range of possibilities for experiments on NIF in this area of material response to extreme conditions.

In summary, new frontiers of HED plasma physics and condensed matter science will be accessible for study on the NIF laser. The coming decade is certain to be punctuated by new discoveries and new understanding of matter at extreme conditions of density and temperature.

ACKNOWLEDGMENTS

This work was performed under the auspices of the Lawrence Livermore National Security, LLC (LLNS) under Contract No. DE-AC52-07NA27344.

¹J. D. Lindl, *Inertial Confinement Fusion: The Quest for Ignition and Energy Gain Using Indirect Drive* (Springer-Verlag, New York, 1998).

²G. H. Miller, E. I. Moses, and C. R. Wuest, *Opt. Eng. (Bellingham)* **43**, 2841 (2004).

³C. A. Haynam, P. J. Wegner, J. M. Auerbach, M. W. Bowers, S. N. Dixit, G. V. Erbert, G. M. Heestand, M. A. Henesian, M. R. Hermann, K. S. Jancaitis, K. R. Manes, C. D. Marshall, N. C. Mehta, J. Menapace, E. Moses, J. R. Murray, M. C. Nostrand, C. D. Orth, R. Patterson, R. A. Sacks, M. J. Shaw, M. Spaeth, S. B. Sutton, W. H. Williams, C. C. Widmayer, R. K. White, S. T. Yang, and B. M. Van Wonterghem, *Appl. Opt.* **46**, 3276 (2007).

⁴J. D. Lindl, *Phys. Plasmas* **2**, 3933 (1995).

⁵J. D. Lindl, P. Amendt, R. L. Berger, S. G. Glendinning, S. H. Glenzer, S. W. Haan, R. L. Kauffman, O. L. Landen, and L. J. Suter, *Phys. Plasmas* **11**, 339 (2004).

⁶E. I. Moses, *J. Phys.: Conf. Ser.* **112**, 012003 (2008); National Ignition Campaign Execution Plan, LLNL Report No. UCRL-AR-213718, 2006; National Ignition Campaign Execution Plan, LLNL Report No. NIF-0111975-AB, 2006.

⁷E. M. Campbell, N. C. Holmes, S. B. Libby, B. A. Remington, and E. Teller, *Laser Part. Beams* **15**, 607 (1997); B. A. Remington and T. S. Perry, "Laser matters: Nova experiments and stockpile stewardship," *Science & Technology Review*, UCRL Report No. UCRL-52000-97-9, pp. 4–13 (September 1997), available from the National Technical Information Service, U.S. Department of Commerce, 5285 Port Royal Road, Springfield, Virginia 22161; https://lasers.llnl.gov/missions/national_security/stockpile_stewardship.php.

⁸T. R. Boehly, R. L. McCrory, C. P. Verdon, W. Seka, S. J. Loucks, A. Babushkin, R. E. Bahr, R. Boni, D. K. Bradley, R. S. Craxton, J. A. Delettrez, W. R. Donaldson, R. Epstein, D. Harding, P. A. Jaanimagi, S. D. Jacobs, K. Kearney, R. L. Keck, J. H. Kelly, T. J. Kessler, R. L. Kremens, J. P. Knauer, D. J. Lonobile, L. D. Lund, F. J. Marshall, P. W. McKenty, D. D. Meyerhofer, S. F. B. Morse, A. Okishev, S. Papernov, G. Pien, T. Safford, J. D. Schnittman, R. Short, M. J. Shoup, M. Skeldon, S. Skupsky, A. W. Schmid, V. A. Smalyuk, D. J. Smith, J. M. Soures, M. Wittman, and B. Yaakobi, *Fusion Eng. Des.* **44**, 35 (1999); <http://www.lle.rochester.edu/>.

⁹D. N. Maywar, J. H. Kelly, L. J. Waxer, S. F. B. Morse, I. A. Begishev, J. Bromage, C. Dorrer, J. E. Edwards, L. Lolnsbee, M. J. Guardalben, S. D. Jacobs, R. Jungquist, T. J. Kessler, R. W. Kidder, B. E. Kruschwitz, S. J. Loucks, J. R. Marciante, R. L. McCrory, D. D. Meyerhofer, A. V. Okishev, J. B. Oliver, G. Pien, J. Qiao, J. Puth, A. L. Rigatti, A. W. Chmid, M. J. Shoup III, C. Stoeckl, K. A. Thorp, and J. D. Zuegel, *J. Phys.: Conf. Ser.* **112**, 032007 (2008); L. J. Waxer, D. N. Maywar, J. H. Kelly, T. J. Kessler, B. E. Kruschwitz, S. J. Loucks, R. L. McCrory, D. D. Meyerhofer, S. F. B. Morse, C. Stoeckl, and J. D. Zeugel, *Opt. Photonics News* **16**, 30 (2005); http://www.lle.rochester.edu/05_omegalaserfacility/05_02_ep/05_ep.php.

¹⁰A. Ng, LLNL Internal Report No. UCRL-TR-52000-07-1/2, 2007, available from the National Technical Information Service, U.S. Department of Commerce, 5285 Port Royal Road, Springfield, Virginia 22161; <http://jlf.llnl.gov/>.

¹¹M. K. Matzen, 2007 IEEE Pulsed Power Conference, 2007, (unpublished), Vols. 1–4, pp. 1–15; M. K. Matzen, M. A. Sweeney, R. G. Adams, J. R. Asay, J. E. Bailey, G. R. Bennett, D. E. Bliss, D. D. Bloomquist, T. A. Brunner, R. B. Campbell, G. A. Chandler, C. A. Coverdale, M. E. Cuneo, J.-P. Davis, C. Deeney, M. P. Desjarlais, G. L. Donovan, C. J. Garasi, T. A. Haill, C. A. Hall, D. L. Hanson, M. J. Hurst, B. Jones, M. D. Knudson, R. J. Leeper, R. W. Lemke, M. G. Mazarakis, D. H. McDaniel, T. A. Mehlhorn, T. J. Nash, C. L. Olson, J. L. Porter, P. K. Rambo, S. E. Rosenthal, G. A. Rochau, L. E. Ruggles, C. L. Ruiz, T. W. L. Sanford, J. F. Seamen, D. B. Sinars, S. A. Slutz, I. C. Smith, K. W. Struve, W. A. Stygar, R. A. Vesey, E. A. Weinbrecht, D. F. Wenger, and E. P. Yu, *Phys. Plasmas* **12**, 055503 (2005); <http://zpinch.sandia.gov/>.

¹²R. P. Johnson, J. Oertel, T. Shimada, F. Archuleta, S. H. Batha, D. M. Esquibel, K. A. Flippo, C. Gautier, R. Gibson, R. P. Gonzales, B. M. Hegelich, C. Hirsche, T. R. Hurry, J. Jorgenson, J. L. Kline, S. Letzinger, F. Lopez, T. Ortiz, S. L. Reid, M. Sorem, and J. C. Fernandez, *J. Phys.:*

- Conf. Ser. (unpublished); N. K. Moncur, R. P. Johnson, R. G. Watt, and R. B. Gibson, *Appl. Opt.* **34**, 4274 (1995); http://www.lanl.gov/orgs/tt/partnering/user_facility/facilities/trident_laser.shtml.
- ¹³D. Besnard, *J. Phys.: Conf. Ser.* **112**, 012004 (2008); J. Ebrardt and J. M. Chaput, *ibid.* **112**, 032005 (2008); A. Bettinger and M. Decroisette, *Fusion Eng. Des.* **46**, 457 (1999); <http://www.google.com/search?hl=en&q=laser+megajoule&start=0&sa=N>.
- ¹⁴M. Dunne, *Nat. Phys.* **2**, 2 (2006); <http://www.hiper-laser.org/>.
- ¹⁵H. Azechi, *J. Phys.: Conf. Ser.* **112**, 012002 (2008); FIREX-I web site: http://www.ile.osaka-u.ac.jp/index_e.html.
- ¹⁶W. Y. Zhang and X. T. He, *J. Phys.: Conf. Ser.* **112**, 302001 (2008); W. Zheng, X. Zhang, X. Wei, F. Jiong, Z. Sui, K. Zheng, X. Yuan, X. Jiang, J. Su, H. Zhou, M. Li, J. Wang, D. Hu, S. He, Y. Xiang, Z. Peng, B. Feng, L. Guo, X. Li, Q. Zhu, H. Yu, Y. You, D. Fan, and W. Zhang, *ibid.* **112**, 032009 (2008); http://english.peopledaily.com.cn/200204/08/eng20020408_93688.shtml.
- ¹⁷M. A. Rhodes, B. Woods, J. J. DeYoreo, D. Roberts, and L. J. Atherton, *Appl. Opt.* **34**, 5312 (1995).
- ¹⁸S. W. Haan, M. C. Herrmann, P. A. Amendt, D. A. Callahan, T. R. Dittich, M. J. Edwards, O. S. Jones, M. M. Marinak, D. H. Munro, S. M. Pollaine, J. D. Salmonson, B. K. Spears, and L. J. Suter, *Fusion Sci. Technol.* **49**, 553 (2006).
- ¹⁹C. P. J. Barty, M. Key, J. Britten, R. Beach, G. Beer, C. Brown, S. Bryan, J. Caird, T. Carlson, J. Crane, J. Dawson, A. C. Erlandson, D. Fittinghoff, M. Hermann, C. Hoaglan, A. Iyer, L. Jones II, I. Jovanovic, A. Komashko, O. Landen, Z. Liao, W. Molander, S. Mitchell, E. Moses, N. Nielsen, H.-H. Nguyen, J. Nissen, S. Payne, D. Pennington, L. Risinger, M. Rushford, K. Skulina, M. Spaeth, B. Stuart, G. Tietbohl, and B. Wattellier, *Nucl. Fusion* **44**, S266 (2004); R. Tommasini, H. S. Park, P. Patel, B. Maddox, S. Le Pape, S. P. Hatchett, B. A. Remington, M. H. Key, N. Izumi, M. Tabak, J. A. Koch, O. L. Landen, D. Hey, A. MacKinnon, J. Seely, G. Holland, L. Hudson, and C. Szabo, *AIP Conf. Proc.* **926**, 248 (2007); H.-S. Park, B. R. Maddox, E. Giraldez, S. P. Hatchett, L. T. Hudson, N. Izumi, M. H. Key, S. Le Pape, A. J. MacKinnon, A. G. MacPhee, P. K. Patel, T. W. Phillips, B. A. Remington, J. F. Seely, R. Tommasini, R. Town, J. Workman, and E. Brambrink, *Phys. Plasmas* **15**, 072705 (2008); https://lasers.llnl.gov/programs/psa/advanced_radiography/.
- ²⁰R. L. McCrory, D. D. Meyerhofer, R. Betti, R. S. Craxton, J. A. Delettrez, D. H. Edgell, V. Yu. Glebov, V. N. Goncharov, D. R. Harding, D. W. Jacobs-Perkins, J. P. Knauer, F. J. Marshall, P. W. McKenty, P. B. Radha, S. P. Regan, T. C. Sangster, W. Seka, R. W. Short, S. Skupsky, V. A. Smalyuk, J. M. Soures, C. Stoeckl, B. Yaakobi, D. Shvarts, J. A. Frenje, C. K. Li, R. D. Petrasso, and F. H. Séguin, *Phys. Plasmas* **15**, 055503 (2008).
- ²¹M. Tabak, J. Hammer, M. E. Glinsky, W. L. Kruer, S. C. Wilks, J. Woodworth, E. M. Campbell, and M. D. Perry, *Phys. Plasmas* **1**, 1626 (1994).
- ²²M. H. Key, *Phys. Plasmas* **14**, 055502 (2007); K. Mima, *J. Phys.: Conf. Ser.* **112**, 012005 (2008).
- ²³SAUUL Workshop, Washington, DC, 17–19 June 2002 (unpublished); http://www.ph.utexas.edu/~utlasers/papers/SAUUL_report.pdf.
- ²⁴*Frontiers in High Energy Density Science, the X-games of Contemporary Science* (National Academies Press, Washington, D.C., 2003).
- ²⁵*Connecting Quarks with the Cosmos: Eleven Science Questions for the New Century* (Committee on the Physics of the Universe, National Research Council, National Academy of Sciences, Washington, D.C., 2003).
- ²⁶*Report of the Interagency Task Force on High Energy Density Physics* (Interagency Task Force on High Energy Density Physics, National Science and Technology Council, Committee on Science, Office of Science and Technology Policy, Washington, D.C., 2007).
- ²⁷B. A. Remington, R. P. Drake, and D. D. Ryutov, *Rev. Mod. Phys.* **78**, 755 (2006).
- ²⁸H. Takabe, *Prog. Theor. Phys. Suppl.* **143**, 202 (2001).
- ²⁹P. Drake, *J. Geophys. Res., [Space Phys.]* **104**, 14505, DOI:10.1029/98JA02829 (1999).
- ³⁰B. H. Ripin, C. K. Manka, T. A. Peyser, E. A. McLean, J. A. Stamper, A. N. Mostovych, J. Grun, K. Kearney, J. R. Crawford, and J. D. Huba, *Laser Part. Beams* **8**, 183 (1990).
- ³¹S. J. Rose, *Laser Part. Beams* **9**, 869 (1991).
- ³²J. A. Koch, N. Izumi, L. A. Welser, R. C. Mancini, S. W. Haan, R. W. Lee, P. A. Amendt, T. W. Barbee, S. Dalhed, K. Fujita, I. E. Golovkin, L. Klein, O. L. Landen, F. J. Marshall, D. D. Meyerhofer, H. Nishimura, Y. Ochi, S. Regan, T. C. Sangster, V. Smalyuk, and R. Tommasini, *High Energy Density Phys.* **4**, 1 (2008).
- ³³H. A. Scott, *J. Quant. Spectrosc. Radiat. Transf.* **71**, 689 (2001).
- ³⁴S. B. Libby, M. Tabak, R. D. Hoffman, M. A. Stoyer, S. W. Haan, S. P. Hatchett, D. P. McNabb, W. E. Ormand, J. Escher, P. Navratil, D. Gogny, M. S. Weiss, M. Mustafa, J. Becker, W. Younes, E. Hartouni, and R. A. Wark, *Inertial Fusion Sciences and Applications—2003*, edited by B. A. Hammel, D. D. Meyerhofer, J. Meyer-ter-Vehn, and H. Azechi (American Nuclear Society, LaGrange Park, IL, 2004), p. 935.
- ³⁵L. J. Suter, S. Glenzer, S. Haan, B. Hammel, K. Manes, N. Meezan, J. Moody, M. Spaeth, and L. Divol, *Phys. Plasmas* **11**, 2738 (2004).
- ³⁶J. C. Niemeyer, W. K. Busche, and G. R. Ruetsch, *Astrophys. J.* **524**, 290 (1999).
- ³⁷B. A. Remington, S. V. Weber, M. M. Marinak, S. W. Haan, J. D. Kilkenny, R. J. Wallace, and G. Dimonte, *Phys. Plasmas* **2**, 241 (1995).
- ³⁸G. Dimonte, C. E. Frerking, M. Schneider, and B. A. Remington, *Phys. Plasmas* **3**, 614 (1996).
- ³⁹V. A. Smalyuk, S. X. Hu, V. N. Goncharov, D. D. Meyerhofer, T. C. Sangster, D. Shvarts, C. Stoeckl, and B. Yaakobi, *Phys. Rev. Lett.* **101**, 025002 (2008).
- ⁴⁰S. W. Haan, *Phys. Rev. A* **39**, 5812 (1989).
- ⁴¹M. M. Marinak, S. G. Glendinning, R. J. Wallace, B. A. Remington, K. S. Budil, S. W. Haan, R. E. Tipton, and J. D. Kilkenny, *Phys. Rev. Lett.* **80**, 4426 (1998).
- ⁴²B. A. Remington, J. Kane, R. P. Drake, S. G. Glendinning, K. Estabrook, R. London, J. Castor, R. J. Wallace, D. Arnett, E. Liang, R. McCray, A. Rubenchik, and B. Fryxell, *Phys. Plasmas* **4**, 1994 (1997).
- ⁴³J. C. Wheeler, J. R. Maund, and S. M. Couch, *Astrophys. J.* **677**, 1091 (2008).
- ⁴⁴K. Kifonidis, T. Plewa, L. Scheck, H.-Th. Janka, and E. Müller, *Astron. Astrophys.* **453**, 661 (2006).
- ⁴⁵D. Ryutov, R. P. Drake, J. Kane, E. Liang, B. A. Remington, and W. M. Wood-Vasey, *Astrophys. J.* **518**, 821 (1999).
- ⁴⁶J. N. Bahcall, W. R. Huebner, S. H. Lubow, P. D. Parker, and R. K. Ulrich, *Rev. Mod. Phys.* **54**, 767 (1982).
- ⁴⁷G. Bazan and D. Arnett, *Astrophys. J.* **496**, 316 (1998).
- ⁴⁸O. R. Pols, K.-P. Schröder, J. R. Hurley, C. A. Tout, and P. P. Eggleton, *Mon. Not. R. Astron. Soc.* **298**, 525 (1998).
- ⁴⁹P. P. Eggleton, D. S. P. Dearborn, and J. C. Lattanzio, *Science* **314**, 1580 (2006).
- ⁵⁰D. S. P. Dearborn, J. C. Lattanzio, and P. P. Eggleton, *Astrophys. J.* **639**, 405 (2006).
- ⁵¹G. Bazan, D. S. P. Dearborn, D. D. Dossa, P. P. Eggleton, A. Taylor, J. I. Castor, S. Murray, K. H. Cook, P. G. Eltgroth, R. M. Cavallo, S. Turcotte, S. C. Keller, and B. S. Pudliner, *ASP Conf. Ser.* **293**, 1 (2003).
- ⁵²W. Dappen, *J. Phys. A* **39**, 4441 (2006).
- ⁵³W. Dappen, *AIP Conf. Proc.* **948**, 179 (2007).
- ⁵⁴C. H. Lin and W. Dappen, *Astrophys. J.* **623**, 556 (2005).
- ⁵⁵T. S. Perry, S. J. Davidson, F. J. D. Serduke, D. R. Bach, C. C. Smith, J. M. Foster, R. J. Doyas, R. A. Ward, C. A. Iglesias, F. J. Rogers, J. Abdallah, Jr., R. E. Stewart, J. D. Kilkenny, and R. W. Lee, *Phys. Rev. Lett.* **67**, 3784 (1991).
- ⁵⁶L. B. Da Silva, B. J. MacGowan, D. R. Kania, B. A. Hammel, C. A. Back, E. Hsieh, R. Doyas, C. A. Iglesias, F. J. Rogers, and R. W. Lee, *Phys. Rev. Lett.* **69**, 438 (1992).
- ⁵⁷P. T. Springer, D. J. Fields, B. G. Wilson, J. K. Nash, W. H. Goldstein, C. A. Iglesias, F. J. Rogers, J. K. Swenson, M. H. Chen, A. Bar-Shalom, and R. E. Stewart, *Phys. Rev. Lett.* **69**, 3735 (1992).
- ⁵⁸J. E. Bailey, G. A. Rochau, C. A. Iglesias, J. Abdallah, Jr., J. J. MacFarlane, I. Golovkin, P. Wang, R. C. Mancini, P. W. Lake, T. C. Moore, M. Bump, O. Garcia, and S. Mazevert, *Phys. Rev. Lett.* **99**, 265002 (2007).
- ⁵⁹R. F. Heeter, J. E. Bailey, M. E. Cuneo, J. Emig, M. E. Foord, P. T. Springer, and R. S. Thoe, *Rev. Sci. Instrum.* **72**, 1224 (2001).
- ⁶⁰L. Ferrarese, H. C. Ford, and W. Jaffe, *Astrophys. J.* **470**, 444 (1996).
- ⁶¹D. A. Liedahl and F. Paerels, *Astrophys. J. Lett.* **468**, L33 (1996).
- ⁶²M. A. Jimenez-Garate, J. C. Raymond, and D. A. Liedahl, *Astrophys. J.* **581**, 1297 (2002).
- ⁶³F. Paerels, J. Cottam, M. Sako, D. A. Liedahl, A. C. Brinkman, R. L. J. van der Meer, J. S. Kaastra, and P. Predehl, *Astrophys. J. Lett.* **533**, L135 (2000).
- ⁶⁴M. E. Foord, R. F. Heeter, P. A. M. van Hoof, R. S. Thoe, J. E. Bailey, M. E. Cuneo, H.-K. Chung, D. A. Liedahl, K. B. Fournier, G. A. Chandler, V. Jonauskas, R. Kisielius, L. P. Mix, C. Ramsbottom, P. T. Springer, F. P.

- Keenan, S. J. Rose, and W. H. Goldstein, *Phys. Rev. Lett.* **93**, 055002 (2004).
- ⁶⁵S. J. Rose, P. A. M. van Hoof, V. Jonauskas, F. P. Keenan, R. Kisielius, C. Ramsbottom, M. E. Foord, R. F. Heeter, and P. T. Springer, *J. Phys. B* **37**, L337 (2004).
- ⁶⁶R. N. Boyd, *An Introduction to Nuclear Astrophysics* (University of Chicago, Chicago, 2008).
- ⁶⁷A. Renzini and F. F. Pecci, *Annu. Rev. Astron. Astrophys.* **26**, 199 (1988); http://en.wikipedia.org/wiki/Globular_cluster.
- ⁶⁸G. Imbriani, H. Costantini, A. Formicola, A. Vomiero, C. Angulo, D. Bemmerer, R. Bonetti, C. Broggini, F. Confortola, P. Corvisiero, J. Cruz, P. Descouvemont, Z. Fulop, G. Gervino, A. Guglielmetti, C. Gustavino, Gy. Gyurky, A. P. Jesus, M. Junker, J. N. Klug, A. Lemut, R. Menegazzo, P. Prati, V. Roca, C. Rolfs, M. Romano, C. Rossi-Alvarez, F. Schumann, D. Schurmamn, E. Somorjai, O. Straniero, F. Strieder, F. Terrasi, and H. P. Trautvetter, *Astron. Astrophys.* **420**, 625 (2004).
- ⁶⁹A. Lemut, D. Bemmerer, F. Confortola, R. Bonetti, C. Broggini, P. Corvisiero, H. Constantini, J. Cruz, A. Formicola, Zs. Fulop, G. Gervino, A. Guglielmetti, C. Gustavino, Gy. Gyurky, G. Imbriani, A. P. Jesus, M. Junker, B. Limata, R. Menegazzo, P. Prati, V. Roca, D. Rogalla, C. Rolfs, M. Romano, C. Rossi-Alvarez, F. Schumann, E. Somorjai, O. Straniero, F. Strieder, F. Terrasi, and H. P. Trautvetter, *Phys. Lett. B* **634**, 483 (2006).
- ⁷⁰M. Busso, R. Gallino, and G. J. Wasserburg, *Annu. Rev. Astron. Astrophys.* **37**, 239 (1999).
- ⁷¹K. Takahashi and K. Yokoi, *At. Data Nucl. Data Tables* **36**, 375 (1987).
- ⁷²Z. Y. Bao, H. Beer, F. Kaeppler, F. Voss, K. Wissak and T. Rauscher, *At. Data Nucl. Data Tables* **76**, 70 (2000).
- ⁷³H. Beer, F. Kappeler, K. Yokoi, and K. Takahashi, *Astrophys. J.* **278**, 388 (1984).
- ⁷⁴K. Wissak, K. Wissak, F. Voss, C. Arlandini, F. Kaeppler, and L. Kazakov, *Phys. Rev. C* **61**, 065801 (2000); K. Wissak, F. Voss, F. Kaeppler, M. Krticka, S. Raman, A. Mengoni, and R. Gallino, *ibid.* **73**, 015802 (2006).
- ⁷⁵J. B. Pollack, A. S. Grossman, R. Moore, and H. C. Grabske, Jr., *Icarus* **30**, 111 (1977); D. Stevenson and E. E. Salpeter, *Astrophys. J., Suppl.* **35**, 239 (1977); A. S. Grossman, J. Pollack, R. Raynolds, A. Summers, and H. Grabske, *Icarus* **42**, 358 (1980).
- ⁷⁶J. J. Fortney and W. B. Hubbard, *Icarus* **164**, 228 (2003).
- ⁷⁷B. J. Conrath, D. Gautier, R. A. Hanel, and J. S. Hornstein, *Astrophys. J.* **282**, 807 (1984); Barney J. Conrath and D. Gautier, *Icarus* **144**, 124 (2000).
- ⁷⁸D. Saumon and T. Guillot, *Astrophys. J.* **609**, 1170 (2004).
- ⁷⁹J. Eggert, S. Brygoo, P. Loubeyre, R. S. McWilliams, P. M. Celliers, D. G. Hicks, T. R. Boehly, R. Jeanloz, and G. W. Collins, *Phys. Rev. Lett.* **100**, 124503 (2008).
- ⁸⁰P. M. Celliers, G. W. Collins, L. B. Da Silva, D. M. Gold, R. Cauble, R. J. Wallace, M. E. Foord, and B. A. Hammel, *Phys. Rev. Lett.* **84**, 5564 (2000).
- ⁸¹P. M. Celliers, G. W. Collins, D. G. Hicks, M. Koenig, E. Henry, A. Benuzzi-Mounaix, D. Batani, D. K. Bradley, L. B. Da Silva, R. J. Wallace, S. J. Moon, J. H. Eggert, K. K. M. Lee, L. R. Benedetti, R. Jeanloz, I. Masclet, N. Dague, B. Marchet, M. Rabec Le Glahec, Ch. Reverdin, J. Pasley, O. Willi, D. Neely, and C. Danson, *Phys. Plasmas* **11**, L41 (2004); *Phys. Rev. Lett.* **69**, 438 (2004).
- ⁸²M. Koenig, E. Henry, G. Huser, A. Benuzzi-Mounaix, B. Faral, E. Martinelli, S. Lepape, T. Vinci, D. Batani, M. Tomasini, B. Telaro, P. Loubeyre, T. Hall, P. Celliers, G. Collins, L. DaSilva, R. Cauble, D. Hicks, D. Bradley, A. MacKinnon, P. Patel, J. Eggert, J. Pasley, O. Willi, D. Neely, M. Notley, C. Danson, M. Borghesi, L. Romagnani, T. Boehly, and K. Lee, *Nucl. Fusion* **44**, S208 (2004).
- ⁸³M. D. Knudson, D. L. Hanson, J. E. Bailey, C. A. Hall, and J. R. Asay, *Phys. Rev. Lett.* **90**, 035505 (2003).
- ⁸⁴D. A. Young, *Phase Diagrams of the Elements* (University of California Press, Berkeley, 1991).
- ⁸⁵R. Ahuja, P. Söderlind, J. Trygg, and J. Melsen, J. M. Wills, B. Johansson, and O. Eriksson, *Phys. Rev. B* **50**, 14690 (1994).
- ⁸⁶P. Söderlind, R. Ahuja, O. Eriksson, B. Johansson, and J. M. Wills, *Phys. Rev. B* **49**, 9365 (1994).
- ⁸⁷J. Edwards, K. T. Lorenz, B. A. Remington, S. Pollaine, J. Colvin, D. Braun, B. F. Lasinski, D. Reisman, J. M. McNaney, J. A. Greenough, R. Wallace, H. Louis, and D. Kalantar, *Phys. Rev. Lett.* **92**, 075002 (2004).
- ⁸⁸K. T. Lorenz, M. J. Edwards, A. F. Jankowski, S. M. Pollaine, R. F. Smith, and B. A. Remington, *High Energy Density Phys.* **2**, 113 (2006).
- ⁸⁹H. S. Park, B. A. Remington, D. Braun, P. Celliers, G. W. Collins, J. Eggert, E. Giraldez, S. Le Pape, T. Lorenz, B. Maddox, A. Hamza, D. Ho, D. Hicks, P. Patel, S. Pollaine, S. Prisbrey, R. Smith, D. Swift, and R. Wallace, *J. Phys.: Conf. Ser.* **112**, 042024 (2008).
- ⁹⁰D. H. Kalantar, J. F. Belak, G. W. Collins, J. D. Colvin, H. M. Davies, J. H. Eggert, T. C. Germann, J. Hawrelia, B. L. Holian, K. Kadau, P. S. Lomdahl, H. E. Lorenzana, M. A. Meyers, K. Rosolankova, M. S. Schneider, J. Sheppard, J. S. Stöcken, and J. S. Wark, *Phys. Rev. Lett.* **95**, 075502 (2005).
- ⁹¹J. Hawrelia, J. D. Colvin, J. H. Eggert, D. H. Kalantar, H. E. Lorenzana, J. S. Stöcken, H. M. Davies, T. C. Germann, B. L. Holian, K. Kadau, P. S. Lomdahl, A. Higginbotham, K. Rosolankova, J. Sheppard, and J. S. Wark, *Phys. Rev. B* **74**, 184107 (2007).
- ⁹²J. S. Wark, R. R. Whitlock, A. A. Hauer, J. E. Swain, and P. J. Solone, *Phys. Rev. B* **40**, 5705 (1989).
- ⁹³J. S. Wark, N. C. Woolsey, and R. R. Whitlock, *Appl. Phys. Lett.* **61**, 651 (1992).
- ⁹⁴J. S. Wark, J. F. Belak, G. W. Collins, J. D. Colvin, H. M. Davies, M. Duchaineau, J. H. Eggert, T. C. Germann, J. Hawrelia, A. Higginbotham, B. L. Holian, K. Kadau, D. H. Kalantar, P. S. Lomdahl, H. E. Lorenzana, M. A. Meyers, B. A. Remington, K. Rosolankova, R. E. Rudd, M. S. Schneider, J. Sheppard, and J. S. Stöcken, *Shock Compression of Condensed Matter*, edited by M. Elert, M. D. Furnish, R. Chau, N. Holmes, and J. Nguyen (AIP, New York, 2005).
- ⁹⁵J. Wark, A. Higginbotham, G. Kimminau, W. Murphy, B. Nagler, T. Whitcher, J. Hawrelia, D. Kalantar, M. Butterfield, B. El-Dasher, J. McNaney, D. Milathianaki, H. Lorenzana, B. Remington, H. Davies, L. Thornton, N. Park, and S. Lukezic, *Shock Compression of Condensed Matter*, edited by M. Elert, M. D. Furnish, R. Chau, N. Holmes, and J. Nguyen (AIP, New York, 2007), p. 1345.
- ⁹⁶B. Yaakobi, F. J. Marshall, T. R. Boehly, R. P. J. Town, and D. D. Meyerhofer, *J. Opt. Soc. Am. B* **20**, 238 (2003).
- ⁹⁷B. Yaakobi, D. D. Meyerhofer, T. Boehly, J. J. Rehr, R. C. Albers, B. A. Remington, and S. M. Pollaine, *Phys. Rev. Lett.* **92**, 095504 (2004); B. Yaakobi, D. D. Meyerhofer, T. Boehly, J. J. Rehr, R. C. Albers, B. A. Remington, P. Allen, and S. M. Pollaine, *Phys. Plasmas* **11**, 2688 (2004).
- ⁹⁸B. Yaakobi, T. R. Boehly, D. D. Meyerhofer, T. J. B. Collins, B. A. Remington, P. G. Allen, S. M. Pollaine, H. E. Lorenzana, and J. H. Eggert, *Phys. Rev. Lett.* **95**, 075501 (2005); *Phys. Plasmas* **12**, 092703 (2005).
- ⁹⁹B. Yaakobi, T. R. Boehly, T. C. Sangster, D. D. Meyerhofer, B. A. Remington, P. G. Allen, S. M. Pollaine, and H. E. Lorenzana, *Phys. Plasmas* **15**, 062703 (2008).
- ¹⁰⁰B. A. Remington, F. Abraham, E. Bringa, M. Ducheneau, J. Edwards, D. Ho, K. T. Lorenz, J. M. McNaney, M. A. Meyers, H. S. Park, S. W. Pollaine, S. T. Prisbrey, R. F. Smith, and B. Yaakobi, High Energy Density Phys. (unpublished).